Space Instrumentation (12)

Lectures for the IMPRS June 23 to June 27 at MPAe Lindau
Compiled/organized by Rainer Schwenn, MPAe,
supported by Drs. Curdt, Gandorfer, Hilchenbach, Hoekzema, Richter, Schühle

Fri, 27.6., 14:00 In-situ instrumentation for planetary surface exploration (Hilchenbach)

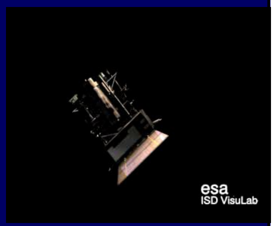

In-situ instrumentation for planetary surface exploration: present and future

M. Hilchenbach

Lindau, June 27, 2003

In-situ instrumentation

instrumentation on the surfaces of
planets, asteroids, moons or comets

- goals:

measurement of elemental and isotopic composition,
mineralogy and soil parameters, geological history,
search for organic compounds on extraterrestrial bodies

- methods:

physical methods and applicable instrument designs:
present and future

Reaching planetary surfaces: example Mars: Entry, descent and landing

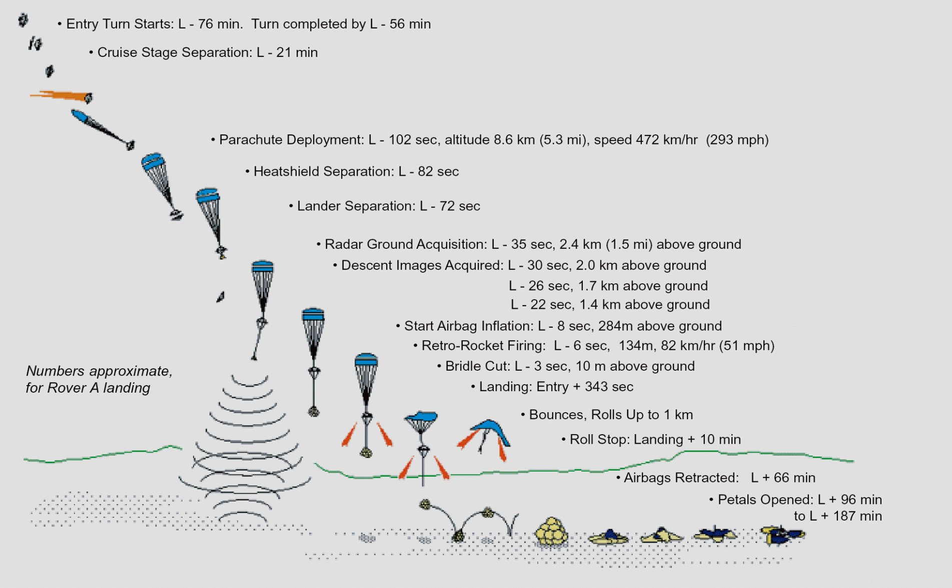

Heavy elements and iron containing minerals

Tools:

APXS - Alpha, Protons and X-ray Sensor
Mössbauer spectrometer

(part of the payload of Nasa`s Martian rover missions Spirit and Opportunity, ESA`s Mars Express lander, Beagle II, ESA’s Rosetta mission)

APXS - Alpha, Protons and X-ray Sensor I

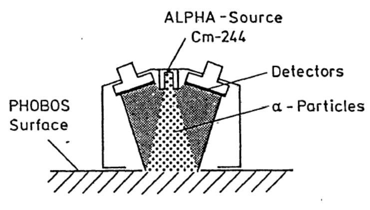

Fig. 1a: ALPHA Sensor

alpha backscattering detector

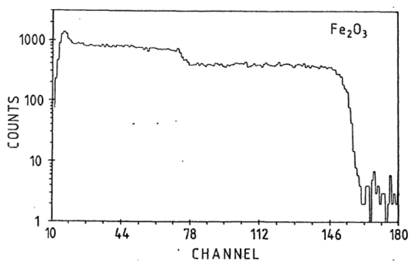

Fig. 2a: Alpha backscattering spectrum from Fe_2O_3 sample taken with a flight instrument.

APXS - Alpha, Protons and X-ray Sensor II

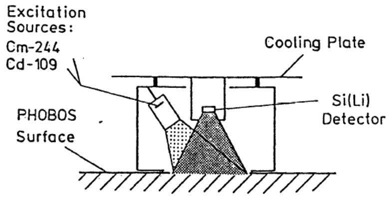

Fig. 1b: X-RAY Sensor

X-Ray fluorescence detector

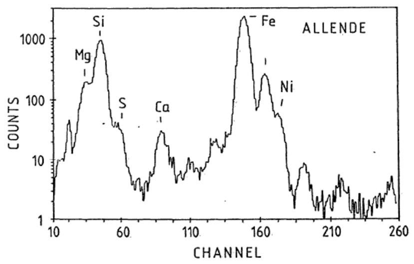

Fig. 2b: X-ray spectrum of Allende meteorite excited by a Cm-244 source and obtained with a flight instrument at detector temperature -110°C.

APXS III - Observations

Mars Pathfinder

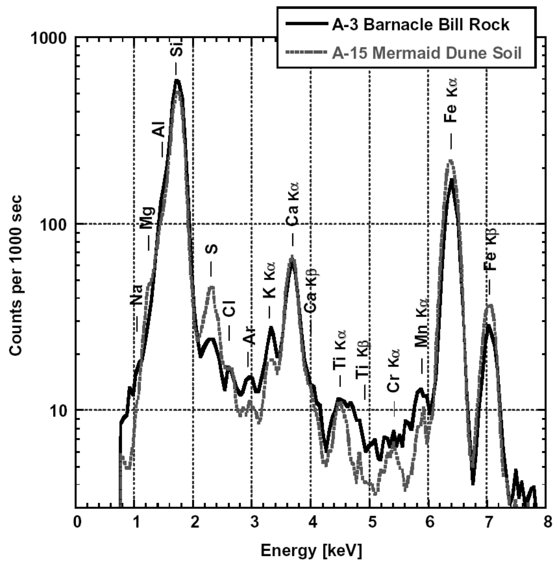

Figure 1 APXS x-ray spectra from Mars Pathfinder landing site: rock 'Barnacle Bill' and soil 'Mermaid Dune'.

Martian and terrestrial sample compositions

Fig. 4. Mg/Si versus Al/Si diagram of martian meteorites (filled triangles), mean values of Viking soils (open diamond), and Pathfinder soils (labeled as MPF soils), as well as Barnacle Bill and calculated "soil-free rock" composition (filled diamonds) in comparison with terrestrial samples.

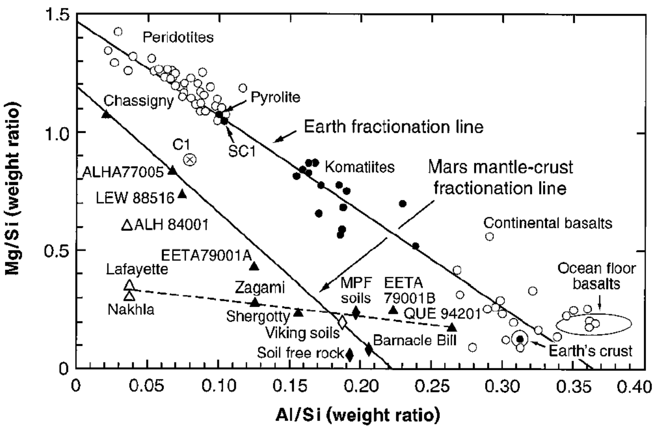

Only the top layer composition is measured

Rieder et al. 1997

Mössbauer spectrometer I

MOSSBAUER SPECTROMETER FOR MARS: G. Klingelhöfer et.al.

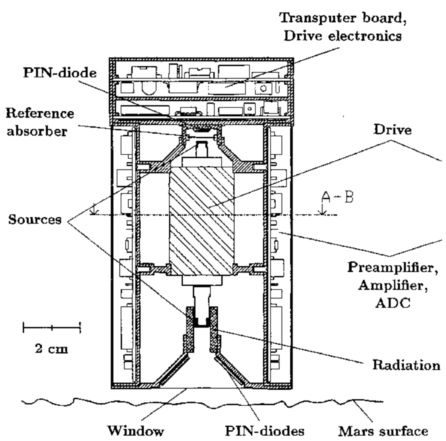

Figure 1: Mössbauer spectrometer for backscattering geometry

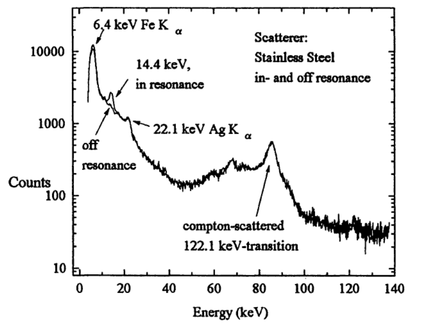

Fig. 2 Energy spectra of backscattered ^{57}Co/Rh radiation, using a prototype of the MIMOS spectrometer.

Mössbauer spectrometer II

Determination of the oxidation state of minerals containing iron

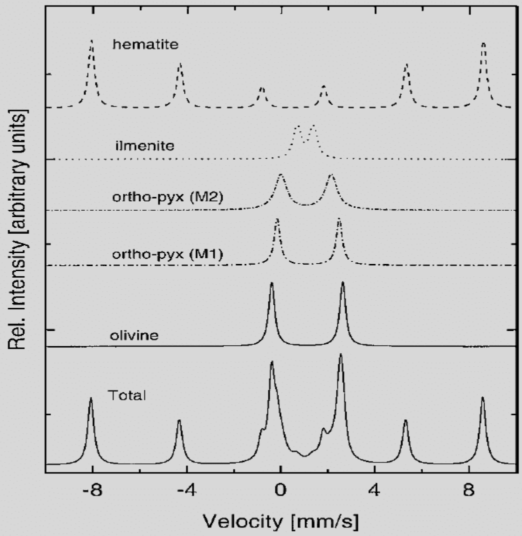

FIG. 1. An example of a calculated backscattering Mössbauer spectrum showing the characteristic subspectra of the different Fe bearing phases and the total spectrum, which is the composite of the subspectra. The same types of lines are used for these minerals in subsequent figures except in the case of the dashed line, which is also used for pyrite and pyrrhotite as noted in the figure captions. See the text for more details.

Sample Acquisition Systems in Space Applications

Lunar Soil - Apollo 15

Apollo Missions Handtools

Tongs (Apollo 12)

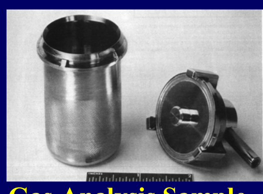

Gas Analysis Sample Container

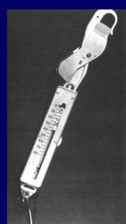

Scale

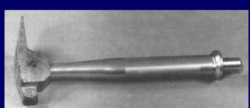

Hammer

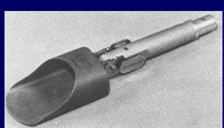

Scoop

Rake (Apollo 16)

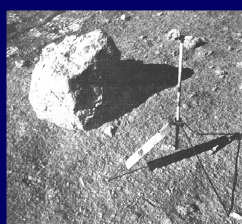

Gnomon (Apollo 15)

Remote Sample Return Missions 30 years ago

Luna 16, 1970

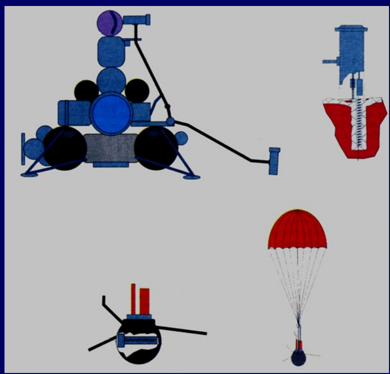

On-orbit dry mass: 5600 kg
Launch Date: 1970-09-12

Drill

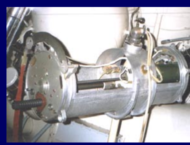

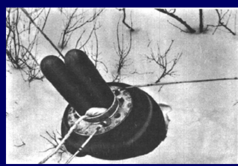

Sealed Capsule

Lunar soil in container: 0.1 kg
Re-entry date: 1970-24-09

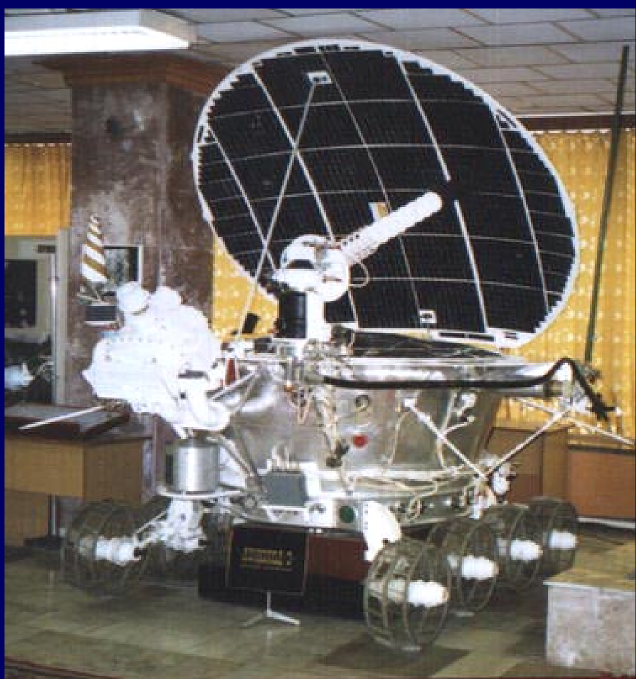

Lunokhod 3

Luna 24, 1976

Example:
"Hard" material: Fractures in individual grains

about 1 mm

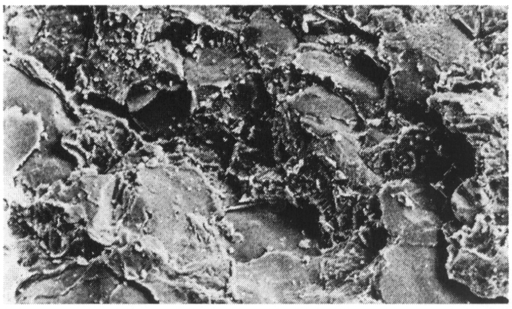

Fig. 23 Hard, quartzitic Bunter sandstone with a very dense and compact fabric. No pores can be seen and the fracture runs through each individual quartz grain ("intragranular failure"; picture length ca. 1 mm)

Sample Acquisition: Mini and Micro Gripper

Micrograppers created in microstructurable glass: Operated by piezo - actor

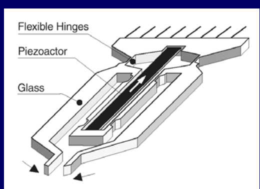

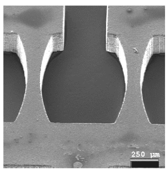

Fig. 2. Solid state hinges of the microgripper

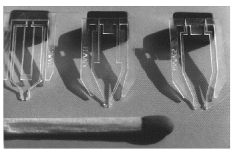

Fig. 3. Various designs of the developed microgrippers

R. Salim et al.
Microsystem Technologies 4, p.32, 1997

Nanotube Nanotweezers: Just voltage operated

P. Kim and C. M. Lieber
SCIENCE 286, p.2148, 1999

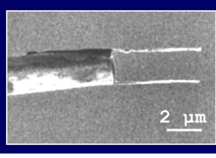

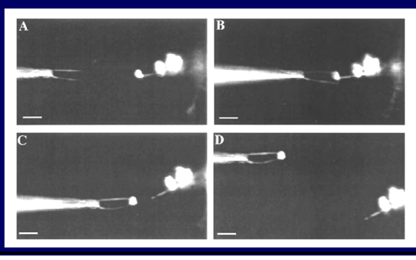

Elements and isotopes

- classification
- objective: elemental and isotopic composition

Tools:
mass spectrometer

Goldschmidt's Classification

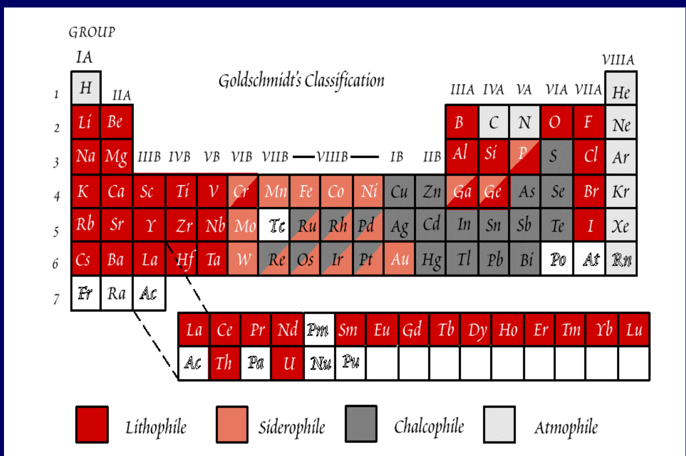

Lithophile: concentration in silicate materials, examples Na, Mg, Al, K or Ca
Siderophile: elements that tend to concentrate in metallic iron, such as Mn or Ni
Chalcophile: elements that concentrate in sulfide phases, examples Cu, Se or Pb
Atmophile: volatile elements in atmospheres, such as H, He or Ar

Objective

Geochemistry of crust and regolith (rocks ?)

Tool: Composition Measurement

Bulk composition of the refractory, lithophile (Al, Ca, Mg, Ti, Be, Sc, V, Sr, Y, Zr, Nb, Ba, REE, Hf, Ta, Th, U), volatile lithophile (K, Na, Rb, Cl, F), refractory siderophile (Fe, Ni, Co, Mo, W), moderately to volatile siderophile or chalcophile (Ga, Ge, Au, Ag and S, Se, Cd, Hg), and atmophile elements (H, He, Ne, Ar, Kr, Xe).

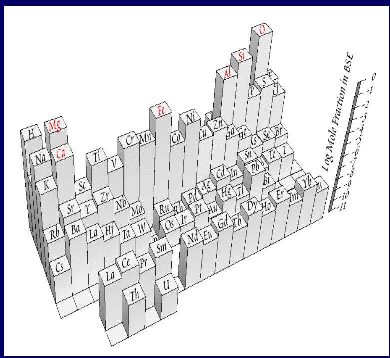

The most abundant elements (99%) are:

O, Mg, Al, Si, Ca, Fe, K, Na

Other element are 'Trace Elements'.

example: 'Bulk Silicate Earth'

Example of Lunar Soil Composition:

i.e. trace elements such as Scandium and Samarium

TABLE 4. Average composition of ropy glasses in 12032 and 12033, with bulk compositions of soils 12032 (Morris *et al.*, 1983) and 12033 (Laul *et al.*, 1980) for comparison. Also given is the major element composition of the quench-crystallized spherule clast (clast number 12032,40-21-1) shown in Figs. 1b and 2d.

	Average 12032,40 Ropy Glass (12032/33)	Std. Dev.	Bulk Soil 12032	Bulk Soil 12033	Bulk Soil -21-1 (Clast)
(Wt%)*					
SiO_2	48.5	(0.41)	46.5	46.9	47.5
TiO_2	2.24	(0.18)	2.9	2.3	0.17
Al_2O_3	15.9	(0.68)	15.2	14.2	23.0
Cr_2O_3	0.20	(0.02)	–	0.39	0.19
FeO	11.4	(0.63)	14.1	15.4	7.27
MnO	0.15	(0.02)	0.20	0.20	0.08
MgO	8.11	(0.41)	9.40	9.20	8.39
CaO	10.7	(0.27)	10.7	11.1	13.2
Na_2O	0.60	(0.13)	0.59	0.67	0.55
K_2O	0.85	(0.21)	0.36	0.41	0.06
P_2O_5	0.74	(0.11)	–	–	0.04
Total	99.6		100.2	100.8	100.5
CaO/ Al_2O_3	0.67		0.70	0.78	0.57
Mg'	0.56		0.54	0.52	0.67
n	51				
(μg/g)**					
Sc	26.8	(2.00)		36.40	
Cr	1506	(217.84)			
Co	19.9	(1.73)		34.30	
Ni	230	(29.96)		130	
Rb	19.1	(2.47)			
Cs	0.68	(0.15)			
Sr	200	(21.35)		160	
Ba	938	(144.78)	529	600	
La	84.8	(13.44)		50	
Ce	220	(33.91)	117	133	
Nd	132	(21.37)	73	85	
Sm	36.9	(6.20)	20.7	22.8	
Eu	2.84	(1.08)		4.9	
Yb	26.4	(3.98)	15.2	17.3	
Lu	3.49	(0.49)	2.24	2.45	
Zr	1232	(160.71)			
Hf	4.48	(2.28)		8.50	
Sb	0.11	(0.06)			
W	1.90	(0.34)			
Ir	<0.01	(0.01)			
Au	0.02	(0.01)			
Zn	37	(6.70)			
n	6				

* Major element oxides for the ropy glasses are from electron microprobe analysis.

** Average minor and trace element abundances (μg/g) of ropy glasses are from INAA data (Table 3).

Wentworth 1994

Trace elements as indicators

Partitioning analysis via trace elements analysis

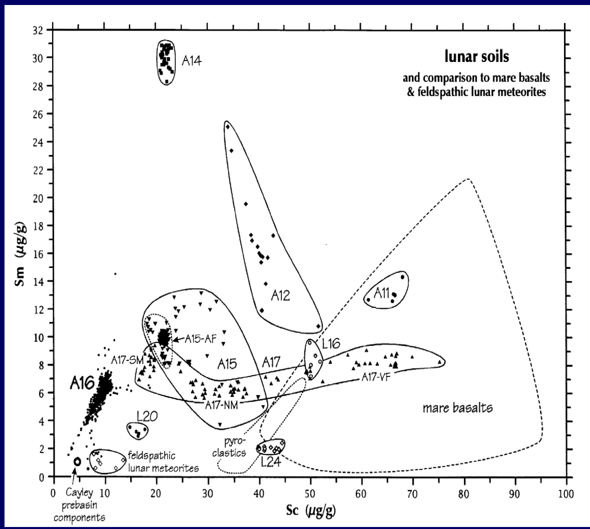

Korotev 1997

Surface history

Surface erosion and “gardening” of surface by impacts

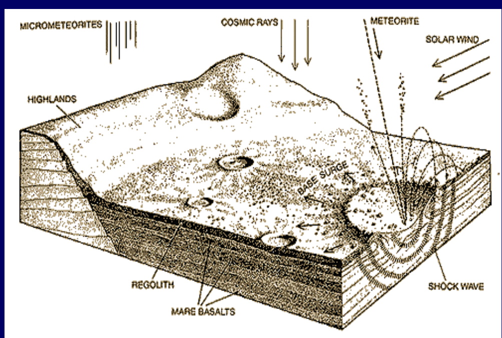

?

Regolith Layer

Impact History
(‘Gardening’)

Method: Identification of
meteorite and cometary
material or solar particles

Measurement of the isotopic ratios

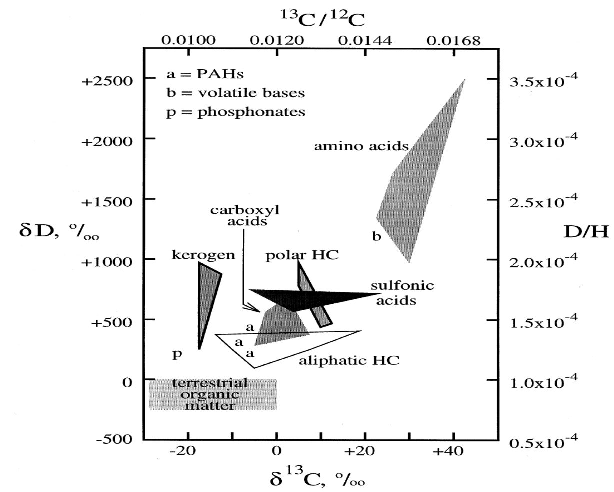

Figure 3. Isotopic ratios for carbon and hydrogen for various molecular compounds from the Murchison meteorite (Cronin and Chang, 1993; and Chang, 1996, private communication). Terrestrial ocean water has by definition $\delta D = 0$ and the cosmic D/H ratio is $(0.8\text{–}2) \times 10^{-5}$ (Irvine and Knacke, 1989).

History - Geochronology

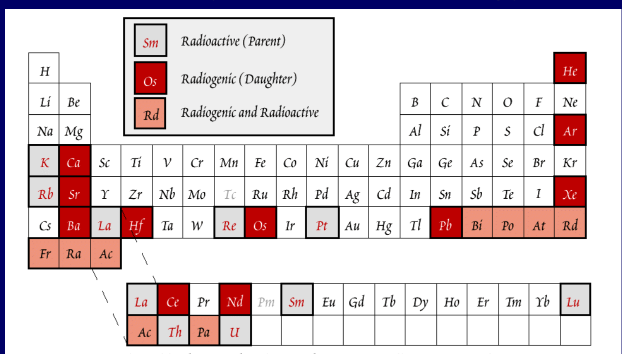

Radiogenic Isotopes Geochemistry

Examples: ^{40}K - ^{40}Ar, ^{87}Rb - ^{87}Sr, ^{147}Sm - ^{143}Nd or ^{182}Hf - ^{182}W (extinct nuclide chronometer)

Presumably not achievable in-situ (lander)….
- required sensitivity
- isobaric interferences

Mass spectrometer instrumentation

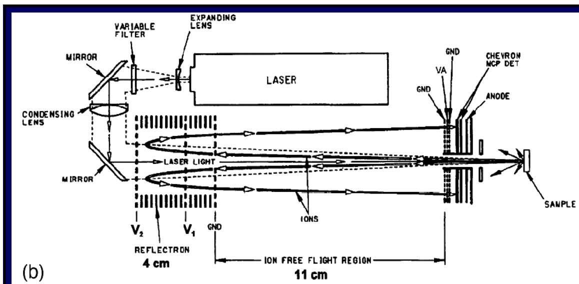

Example: "In situ" mass spectrometry

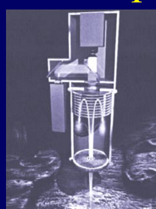

Laser desorption source and refectron type time-of-flight. Mass ~2 kg, Volume ~20x15x10 cm^3

W. B. Brinckerhoff, APL
G. G. Managadze, IKI
2000

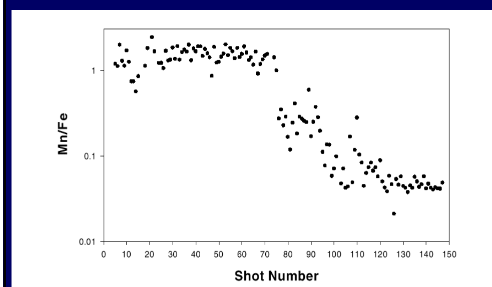

Mn/Fe ratio versus shot number

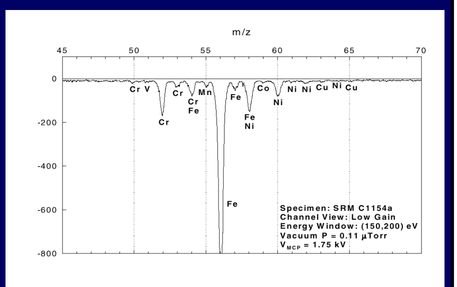

Basalt: Mass spectrum Fe, Cr isotopes

E||B Energy-Mass Spectrograph for Measurement of Ions and Neutral Atoms

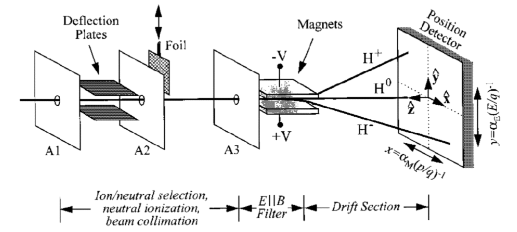

FIG. 1. **E**||**B** spectrograph for measurement of ion and neutral atom mass-per-charge and energy-per-charge distributions.

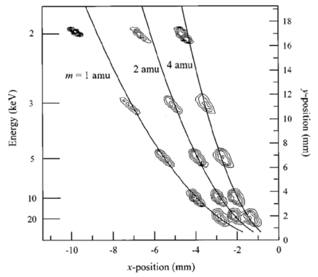

FIG. 3. Spectrograph of H^+, H_2^+, and $^4He^+$ beams incident at 2, 3, 5, 10, and 20 keV. Each contour line represents linear increments of 200 counts. The data closely follows the empirical fit of Eqs. (1) and (2) (solid lines).

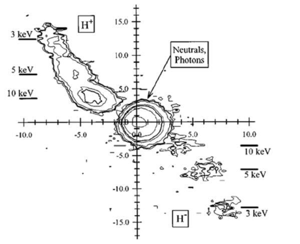

FIG. 4. Spectrograph of 3, 5, and 10 keV H after transiting a nominal 1 $\mu g/cm^2$ carbon foil, simulating neutral atom measurements. Contours are logarithmically spaced. Positive and negative ions are observed in the second and fourth quadrants, respectively. Neutral atoms exiting the foil are observed in the center of the detector; photons that can stimulate the detector would also be observed in the center of the detector.

Funsten 1996

Hadamard transform time-of-flight mass spectrometer

High duty cycle: about 50%

Rev. Sci. Instrum., Vol. 71, No. 3, March 2000

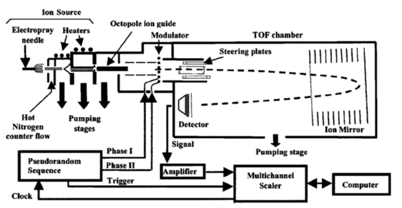

1308 Rev. Sci. Instrum., Vol. 71, No. 3, March 2000

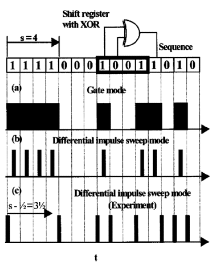

FIG. 1. Operational modes of the Hadamard transform time-of-flight mass spectrometer. The sequence generated by a four-bit shift register with XOR feedback of bits three and two is shown at the top. (a) Gate mode and unit time resolution, (b) differential impulse sweep mode, and (c) modulation function used in the experiment. The introduced phase shift $s-\frac{1}{2}=3\frac{1}{2}$ sequence elements between gate and differential impulse sweep mode is indicated (s is the distance between the largest blocks of consecutive 1's and 0's in the sequence).

Brock 1999

1312 Rev. Sci. Instrum., Vol. 71, No. 3, March 2000

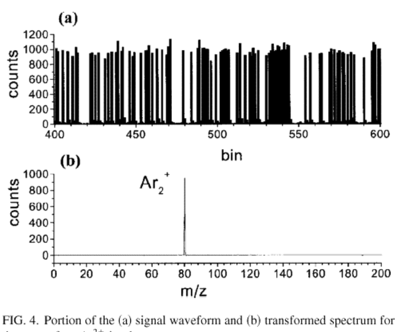

FIG. 4. Portion of the (a) signal waveform and (b) transformed spectrum for the case of an Ar^{2+} ion beam.

Mass spectroscopy using a rotating electric field

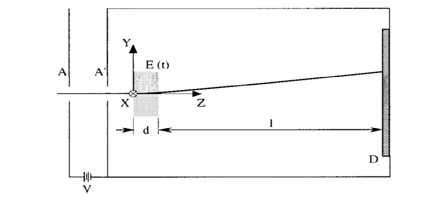

FIG. 1. Schematic of the REFIMS showing apertures A and A′, region of time-dependent electric field (shaded), and position-sensitive detector D. The bias voltage V accelerates ions into the analyzer. Also shown is the coordinate system used and the geometrical parameters l and d. Cylindrical symmetry about the z axis is implied.

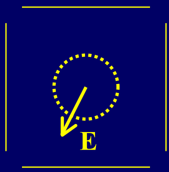

time-of-flight → phase

Rev. Sci. Instrum., Vol. 69, No. 6, June 1998

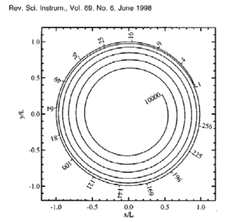

FIG. 2. Locus of points in the r-α plane for masses spanning the range 1–10 000 amu. This is the coordinate system that rotates with the direction of the deflection field, not one that is fixed in the laboratory frame. Here $l = 10\ d$ and $\omega = 0.4\ \omega_0$. Tick marks on the curve indicate the positions of several masses (in amu).

J. H. Clemmons and F. A. Herrero

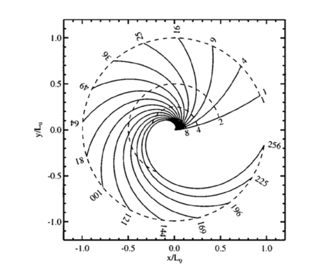

FIG. 7. r-α plane for several indicative masses between 1 and 256 amu (solid lines) for the energy range 1–100 ϵ. Broken traces indicate the positions of several energies (in units of ϵ). (After Fig. II.21 of Ref. 7.)

Clemmons 1998

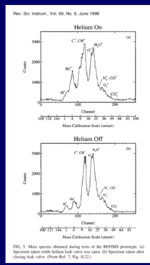

Technology: Surface microstructure/miniature mass spectrometer

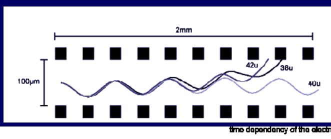

Siebert, 1998

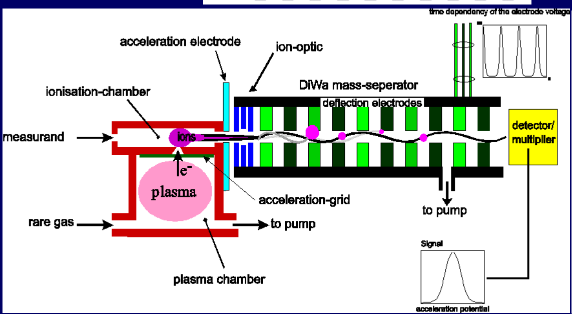

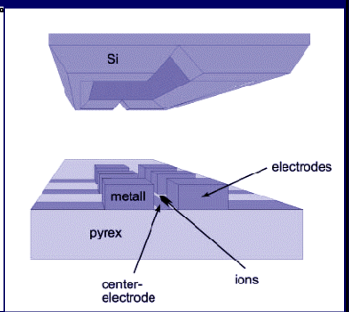

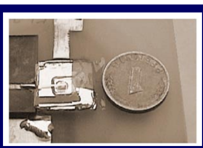

Manufacturing by lithographic
3D techniques (e.g. LIGA)

Electrostatic Axially Harmonic Orbital Trapping: A High-Performance Technique of Mass Analysis

A. Makarov 2000

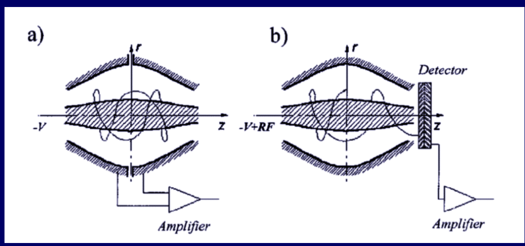

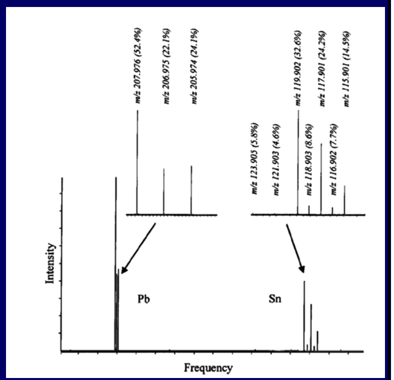

Modes of operation:
a) Fourier transform
b) mass selective instability

Mass spectrum in frequency domain

A Capacitance Standard Based on Counting Electrons

'Quantum dots'

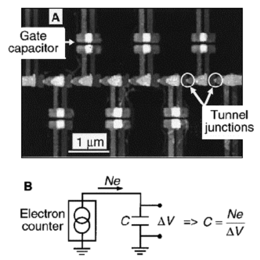

Fig. 1. (A) Scanning force microscope image of a seven-junction electron pump. The device consists of two layers of Al shifted horizontally by ≈0.2 μm to form tunnel junctions at the bright spots where the tip of each island overlaps its neighbor to the left. Pulsing the gates in sequence from left to right transfers electrons from left to right, and vice versa. After N cycles, the charge transferred through the pump is Ne, with an uncertainty of 1 part in 10^8. (B) Schematic implementation of the definition of capacitance by counting electrons.

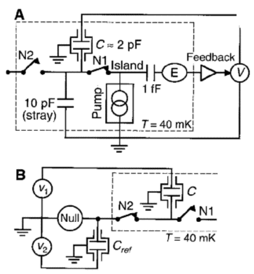

Fig. 2. Schematic diagram of the SET capacitance standard. (A) Configuration used to pump electrons onto C. The stray capacitance of 10 pF comes mostly from the third terminal of the vacuum-gap capacitor. (B) Configuration used to compare C with another capacitor at room temperature using an ac bridge.

Temperature 40 mK

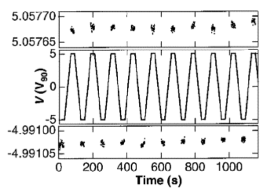

Fig. 3. Voltage applied to the capacitor by the feedback circuit while pumping electrons on and off C. Expanded views of the plateaus are shown above and below the main plot. For these data, N = 117 440 513 (= 7000001 hexadecimal) and $\langle \Delta V \rangle$ = 10.048 703 31 V_{90}, giving C = 1.872 484 77 pF from Eq. 2.

Keller 1999

Mineralogy

Tools

- (infrared spectrometer)
- **Raman spectrometer**

Illustration (Moon)

Landscape, Apollo 15

scale: 80 mm

"Close-up" Lunar soil, Apollo 12

scale: 1 mm

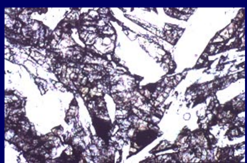

Photomicrograph of lunar basalt, Apollo 16

scale: 2.5 mm

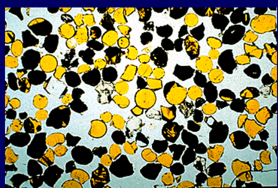

Orange volcanic glass (lava) and ilmenite ($FeTiO_3$), Apollo 17

Geochemistry:

Minerals Typically Found In Lunar Regolith (From Williams And Judwick, 1980)

Major	Minor
Olivine $(Mg,Fe)_2SiO_4$	Spinels $(Fe,Mg,Al,Cr,Ti)O_4$
Pyroxene $(Ca,Mg,Fe)SiO_3$	Armalcolite (Fe_2TiO_5)
Plagioclase feldspars $(Ca,Na)Al_2Si_2O_8$	Silica (quartz, tridymite, cristobalite) SiO_2
	Iron Fe (variable amounts of Ni and Co)
	Troilite FeS
	Ilmenite $FeTiO_3$

Trace

Phosphates	Oxides
Apatite[a] $Ca_5(PO_4)_3(F,Cl)_3$	Rutile TiO_2
Whitlockite[a] $Ca_9(Mg,Fe)(PO_4)_7(F,Cl)$	Corundum (?) Al_2O_3
	Hematite (?) Fe_2O_3
	Magnetite Fe_3O_4
	Goethite (?) FeO(OH)
Zr mineral	**Metals**
Zircon[a] $ZrSiO_4$	Copper (?) Cu
Baddeleyite ZrO_4	Brass (?)
	Tin (?) Sn
Silicates	**Zr-rich mineral**
Pyroxferroite $(Fe,Mg,Ca)SiO_3$	Zirkilite or zirconolite[a] $CuZrTi_2O_7$
Amphibole $(Ca,Mg,Fe)(Si,Al)_8O_{22}F$	
Garnet (?)	
Tranquilletyite[a] $Fe_8Zr_2Ti_3Si_3O_4$	
Sulfides	**Meteoritic minerals**
Mackinawite $(Fe,Ni)_9S_8$	Schreibernite$(Fe,Ni)_3$
Pentlandite $(Fe,Ni)_9S_8$	Cohenite (Fe,Ni,Co),O
Cubanite $CuFe_2S_3$	Niningerite (Mg,Fe,Mn)S
Chalcopyrite $CuFeS_2$	Lawrencite (?) $(Fe,Ni)Cl_2$
Sphalerite (Zn,Fe)S	

[a]These minerals are known to exhibit complex substitutions, particularly of elements as Y, Nb, Hf, U, and the rare earth elements that are concentrated in these minerals.

Minerals in the lunar regolith

Principles of Raman spectroscopy

scattering system with
quantizied eigenstates E_f-E_i
$\hbar \nu_R = E_f - E_i$

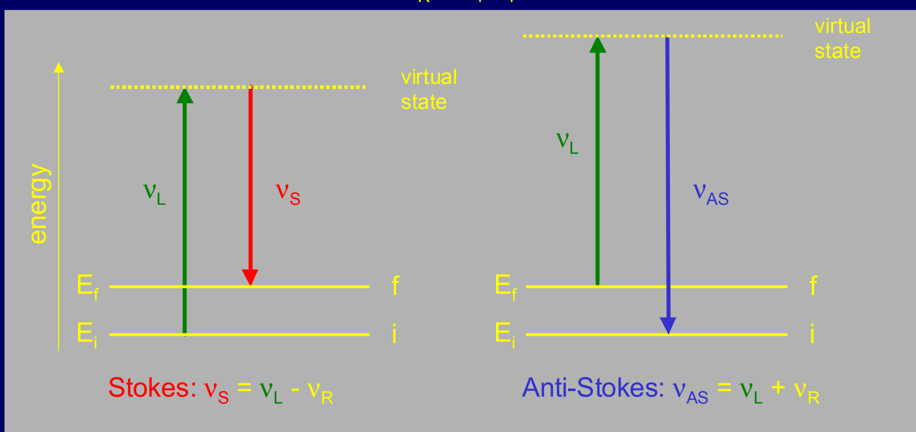

Principles of Raman spectroscopy

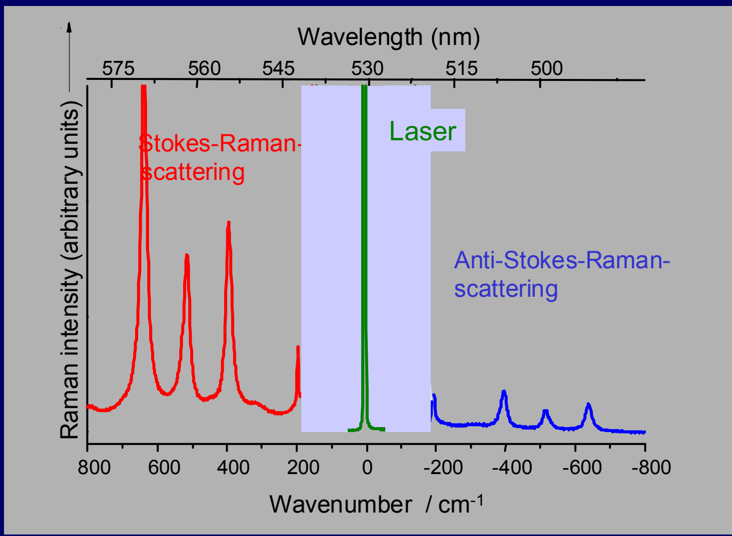

"In-situ" Mineralogy: Structure (and Composition)

….
Oxides Sulphides
Feldspars Silicates
Meteoritic Minerals
….

Example → Olivine - Series between two end-members: Forsterite (Mg_2SiO_4) and Fayalite (Fe_2SiO_4),

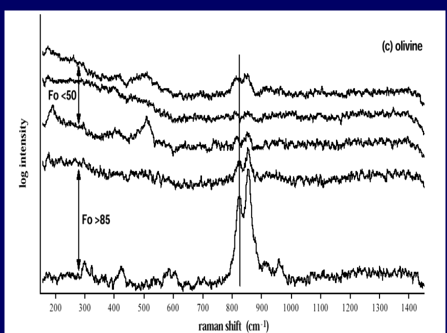

Example: Lunar regolith (Apollo 17 "Sample Return")
Position of 820 cm^{-1} peak shifts with Mg/Fe ratio
Raman Spectrometry, Korotev 1997

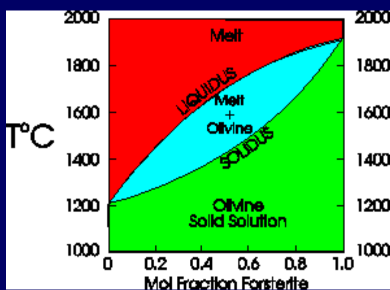

Olivine - Temperature, phase and molecular fractionation

Organic compounds

Goals

identification and quantification of
- traces of organic compounds in the Martian deep soil
- organic compounds in the surface matter of a comet

Tool

- gas chromatograph coupled with a mass spectrometer

Viking 1976

Result: no life detected, could not even identify organic molecules (< ppb) in the upper layer of the Martian soil.

Science goal: Signs of Past and Present Life

Are there any organic or water molecules in the Martian soil or atmosphere ?

Detection and determination of organic compounds and water in Martian soil from different depths

- Observation of oxidised organic compounds, not just CO_2 ; Question: What are the oxidising agents ? Are they present in the deeper Martian soil layers ?

- Identification and characterisation of minute traces of complex organic molecules, which might be contained and/or encapsulated in the subsurface material and are most likely very rare. Amino acid chirality determination.

- Determination of elements essential for (terrestrial) life, such as C, O, N and H

- Measurement of the isotopic ratios, such as D/H, ^{13}C /^{12}C, ^{15}N/^{14}N etc.

- Traces of extinct life forms, even more interesting, traces of extant life forms

Goal: identification and quantification of traces of organic compounds

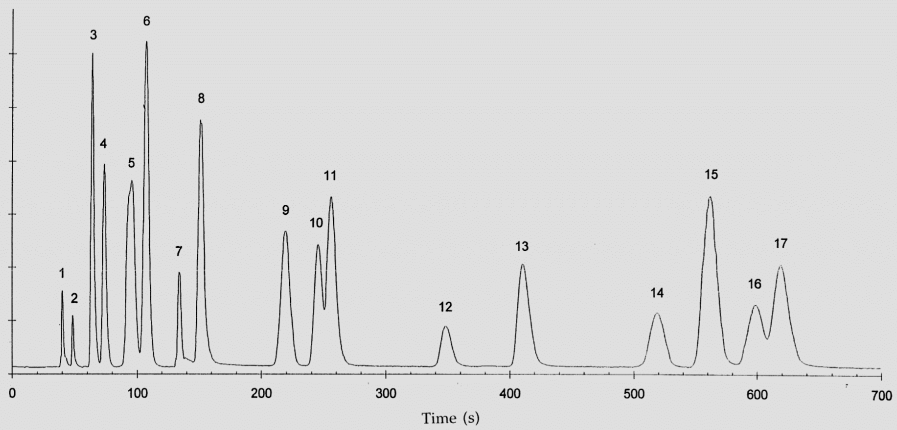

Fig. 4. Chromatogram of a mixture of hydrocarbons (C_1 to C_6) and nitriles (C_1 to C_4) with a CPP–DMPS (14:86) capillary column. Capillary column MXT 1701 (10 m×0.18 I.D. mm). MS ion trap detector as in Ref. [16]. Carrier gas, He; temperature, 30°C; pressure drop, 0.3 bar. (1) Methane, (2) 1-butene, (3) *n*-pentane+1-pentene, (4) 2-methyl-2-butene, (5) cyclopentane+3-methylpentane, (6) *n*-hexane+1-hexene, (7) acetonitrile, (8) acrylonitrile, (9) *n*-heptane+cyclohexene, (10) benzene+methacrylonitrile, (11) propionitrile, (12) iso-butyronitrile, (13) *cis*- or *trans*-crotonitrile, (14) *n*-octane, (15) butyronitrile, (16) toluene, (17) *cis*- or *trans*-crotonitrile.

GC-MS:
Gas chromatograph coupled to mass spectrometer

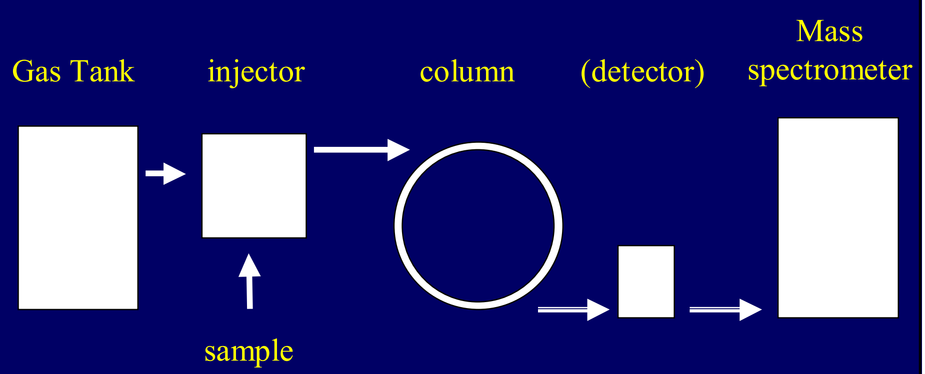

Schematic view

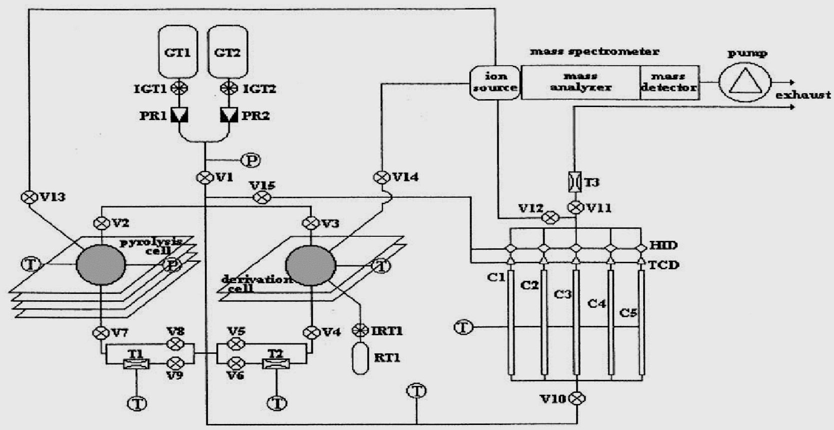

GT1-2	gas tank
RT1-2	reagent tank
IGT1-2	isolation valve for gas tank ⊛
IRT1-2	isolation valve for reagent tank
PR1-2	pressure regulator
P, T	presure and temperature sensors Ⓟ Ⓣ
V1-15	on/off valve ⊗
T1-3	trap
C1-5	GC column
TCD1-5	thermal conductivity detector △
HID1-5	helium ionisation detector ◇

Identification and characterisation of minute traces of complex organic molecules

HPLC analyis

Glavin 1999

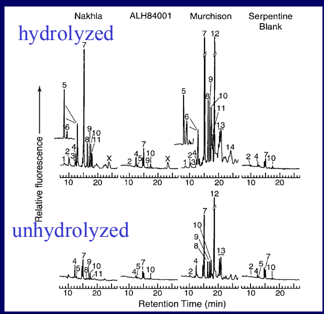

Table 1. Expected Metastable Products from Organic Substances in the Murchison meteorite[5,6]

Substance	Concentration (parts per million)	Metastable Products
Acid insoluble kerogen	14500	Benzenecarboxylic acids
Aliphatic hydrocarbons	12–35	Acetate
Aromatic hydrocarbons	15–28	Benzenecarboxylic acids
Monocarboxylic acids	≈330	Acetate/oxalate
2-Hydroxycarboxylic acids	14.6	Acetate/carbonate
Alcohols (primary)	11	Acetate
Aldehydes	11	Acetate
Ketones	16	Acetate, benzenecarboxylic acids
Amines	10.7	Acetate
Urea	25	Carbonate
Heterocycles	12	Carbonate, other products

Benner 2000

Sample preparation and sample concentration is required prior to the GC-MS analysis.

A GC-MS can only analyze volatile compounds.

Most metastable products of organics substances are refractory (e.g. salts). The sample preparation (e.g. esterification) is an essential condition for the GC-MS analysis.

Chemical derivatization

PRINCIPLE :

organic molecule + derivatizing agent → derived compound

OBJECTIVES :

Less polar or more volatile molecules

Increased sensitivity and better separation

EXAMPLES :

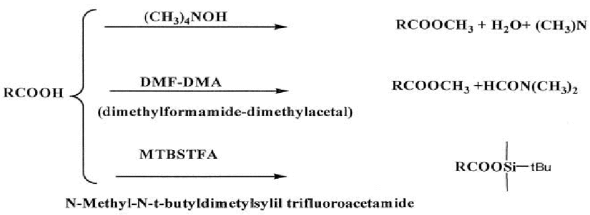

Fig. 3. Illustration of chemical derivatization (CD) principle and examples of one-step reactions commonly used in laboratory that could fulfill all our requirements. The carboxylic acid on the left side of the reaction scheme is derivatized using three different reactions. This leads, from top to bottom, to different esters, which can be easily analyzed by conventional means.

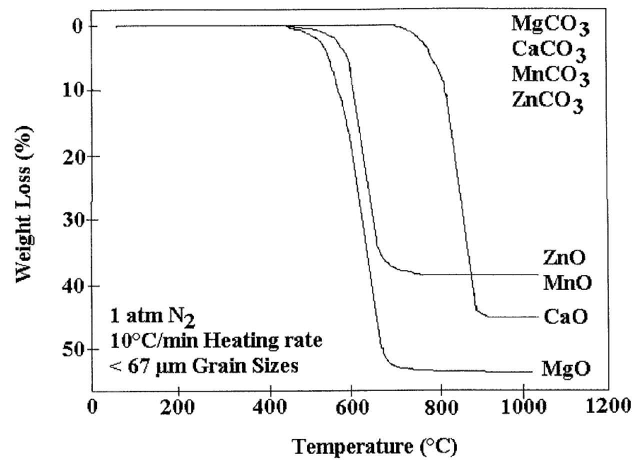

Fig. 1. The thermal stabilities of mineral phases and their volatile release profiles were studied by conventional thermogravimetric analysis. Here are presented decomposition of magnesite, calcite, rhodochrosite and smithsonite at heating rates of up to 10°C/min. Pyrolysis experiments results, at heating rates much faster, are also available in the original article (adapted from Kotra et al., 1982).

Pyrolysis cell

Cassini`-Huygens visit to the atmosphere of Saturn`s moon Titan

Table 1
Chemical composition of Titan's atmosphere (adapted from Ref. [6])[a]

Detected compounds			Expected compounds		
	Stratospheric mixing ratio	Simulation experiment	Hydrocarbons	Nitriles	O-Compounds
N_2	0.90–0.99				
Ar	<0.06				
CH_4	0.017–0.045				
	0.017–0.12 T				
CO	5.0×10^{-5}				HCHO
CO_2	1.3×10^{-8} N				CH_3OH
H_2	0.00060–0.0014				
H_2O	8.0×10^{-9}				
C_2H_6	1.6×10^{-5} N	Maj.	Propene		
C_2H_2	6.5×10^{-6} N	Maj.	Allene		
C_2H_8	1.2×10^{-6} N	++	Cyclopropane		
C_2H_4	1.5×10^{-5} N	++	Triacetylene		
C_3H_4	3.7×10^{-8} N	+	Tetraacetylene		
C_4H_2	2.7×10^{-8} N	+	C_4H_4		
HCN	1.5×10^{-6} N	Maj.	1,2-C_4H_6	C_2H_5–CN	
HC_3N	4.5×10^{-8} N	++	1,3-C_4H_6	CH_2=CH–CN	
C_2N_2	2.2×10^{-8} N	+	C_4H_8	CH_3–C_2–CN	
CH_3CN	Detected	++	*n*-C_4H_{10}	*n*-C_3H_7–CN	
C_4N_2	Solid phase		iso-C_4H_{10}	iso-C_3H_7–CN	
			C_6H_6	cyclo-C_3H_6–CN	
				HC_5N	

[a] T, troposphere; N, north pole.

GC-MS onboard the Rosetta Lander

Gas chromatograph coupled to high resolution mass spectrometer

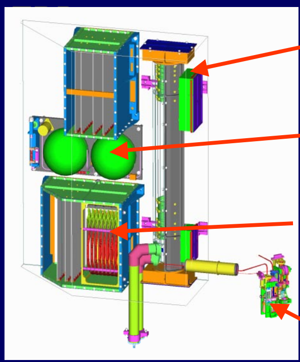

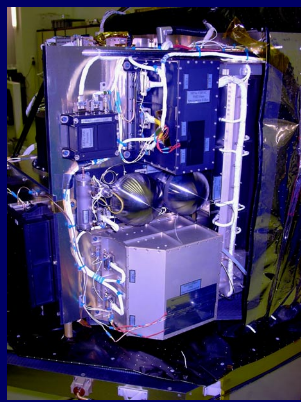

Example: COSAC (Rosetta Lander 2003)

New target : 67P/Churyumov-Gerasimenko

Rolando Ligustri
February 1st 2003

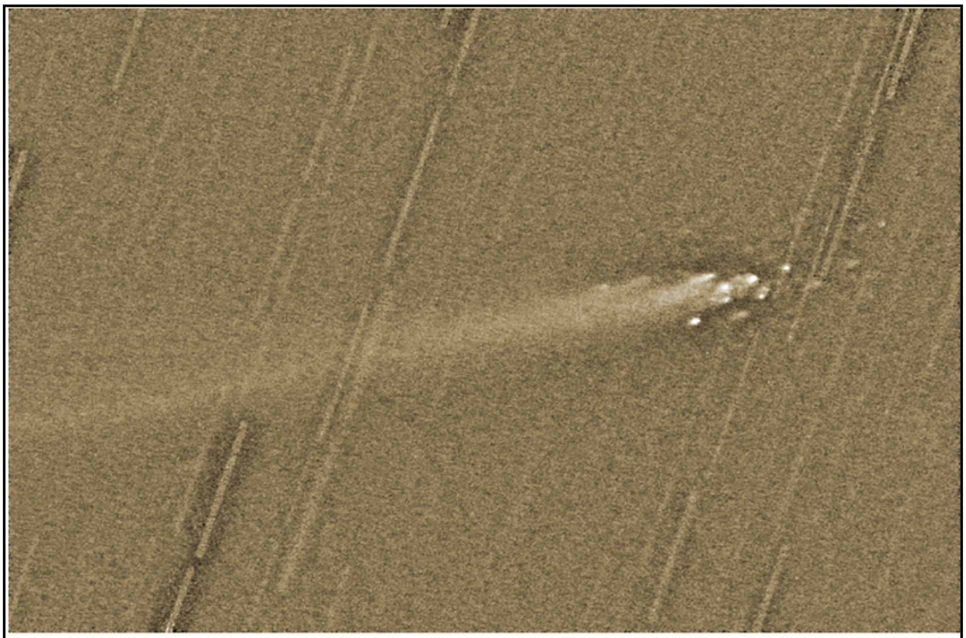

Break-up of Comet Linear (C/1999 S4)
(VLT ANTU + FORS-1)

ESO PR Photo 20/00 (8 August 2000)

In-situ measurements on the comet surface

Experiments on the Rosetta Lander

Images (CIVA, ROLIS), in-situ analysis (APX, COSAC, PTOLEMY), electrical and acustical measurements, temperature and dust (MUPUS, SESAME), magnetic field and plasma, radiowavestransmission - „nucleus-tomographie“ (ROMAP, CONSERT)

Drilling and Destruction: Material strength and Work

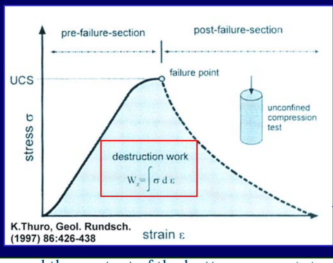

Design requirement drivers:
- Wearing of drill bit
- Contamination of drill sample

Around the contact of the button a new state of stress is induced in the rock, where four important destruction mechanisms can be distinguished:

1. Under the bit button a crushed zone of fine rock powder is formed (impact).
2. Starting from the crushed powder zone, radial cracks are developed (induced tensile stress).
3. When stress in the rock is high enough (if enough cracks exist ± parallel to the bottom of the borehole), larger fragments of the rock can be sheared off between the button grooves (shear stress).
4. In addition to the mechanisms above, stress is induced periodically (dynamic process).

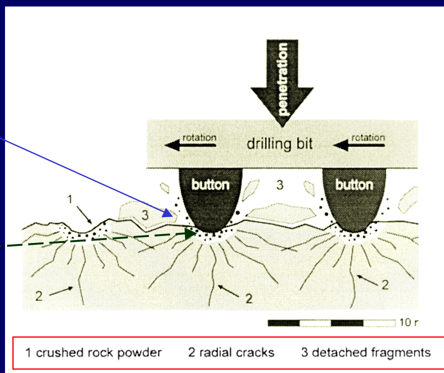

Fig. 12 Crushing process in rotary percussive drilling. Destruction mechanism under the bit buttons

Ad possible instrumentation for Mars:

Ion Mobility Spectrometer

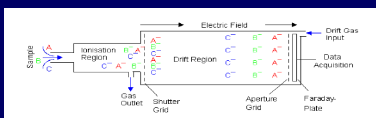

Principle of operation:
Ion Mobility Spectrometer

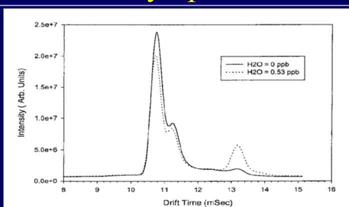

Figure 2. Mobility spectrum for getter-purified N_2 with and without the addition of 0.53 ppb H_2O.

Ion mobility spectrum (H_2O)

Figure 1: Drift tubes of different size: conventional (left), miniaturized (right)

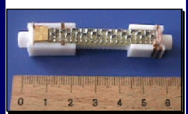

Figure 2: Dimensions of a miniaturized and mass producible drift tube of an IMS

Miniature drift tubes

S. N. Ketkar et al., Anal. Chem.2001, 73, 2554-2557
Teepe, M. et al. Proceedings of the VDE World Micro-Technologies Congress, Expo2000, Hannover 2 (2000) 547-549

25 elements essential for (terrestrial) life

Group 1	Group 2	Group 3	Group 4	Group 5	Group 6	Group 7	Group 8
Hydrogen 1 H							Helium 2 He
Lithium 3 Li	Beryllium 4 Be	Boron 5 B	Carbon 6 C	Nitrogen 7 N	Oxygen 8 O	Fluorine 9 F	Neon 10 Ne
Sodium 11 Na	Magnesium 12 Mg	Aluminium 13 Al	Silicon 14 Si	Phosphorus 15 P	Sulphur 16 S	Chlorine 17 Cl	Argon 18 Ar
Potassium 19 K	Calcium 20 Ca	Gallium 31 Ga	Germanium 32 Ge	Arsenic 33 As	Selenium 34 Se	Bromine 35 Br	Krypton 36 Kr
Rubidium 37 Rb	Strontium 38 Sr	Indium 49 In	Tin 50 Sn	Antimony 51 Sb	Tellurium 52 Te	Iodine 53 I	Xenon 54 Xe
Caesium 55 Cs	Barium 56 Ba	Thallium 81 Tl	Lead 82 Pb	Bismuth 83 Bi	Polonium 84 Po*	Astatine 85 At*	Radon 86 Rn*
Francium 87 Fr*	Radium 88 Ra*	(113)					

*Radioactive

Transition Elements

Scandium 21 Sc	Titanium 22 Ti	Vanadium 23 V	Chromium 24 Cr	Manganese 25 Mn	Iron 26 Fe	Cobalt 27 Co	Nickel 28 Ni	Copper 29 Cu	Zinc 30 Zn
Yttrium 39 Y	Zirconium 40 Zr	Niobium 41 Nb	Molybdenum 42 Mo	Technetium 43 Tc*	Ruthenium 44 Ru	Rhodium 45 Rh	Palladium 46 Pd	Silver 47 Ag	Cadmium 48 Cd
Lanthanum 57 La	Hafnium 72 Hf	Tantalum 73 Ta	Tungsten 74 W	Rhenium 75 Re	Osmium 76 Os	Iridium 77 Ir	Platinum 78 Pt	Gold 79 Au	Mercury 80 Hg
Actinium 89 Ac*	(104)								(112)

Building blocks for DNA (highlighted: H, C, N, O, P)

Berlow, Burton and Routh, 1974

Lanthanide and Actinide Series

Cerium 58 Ce	Praeseodymium 59 Pr	Neodymium 60 Nd	Promethium 61 Pm*	Samarium 62 Sm	Europium 63 Eu	Gadolinium 64 Gd	Terbium 65 Tb	Dysprosium 66 Dy	Holmium 67 Ho	Erbium 68 Er	Thulium 69 Tm	Ytterbium 70 Yb	Lutetium 71 Lu
Thorium 90 Th*	Protactinium 91 Pa*	Uranium 92 U*	Neptunium 93 Np*	Plutonium 94 Pu*	Americum 95 Am*	Curium 96 Cm*	Berkelium 97 Bk*	Californium 98 Cf*	Einsteinium 99 Es*	Fermium 100 Fm*	Mendelevium 101 Md*	Nobelium 102 No*	Lawrenciu 103 Lr*

*Radioactive (elements after 92 artificially created)

Ultrasonic Coring Device

Sample contamination avoidance: No medium (fluid, mud) should be added to corer - soil interface

About 30 W power requirement, depth about 10 cm

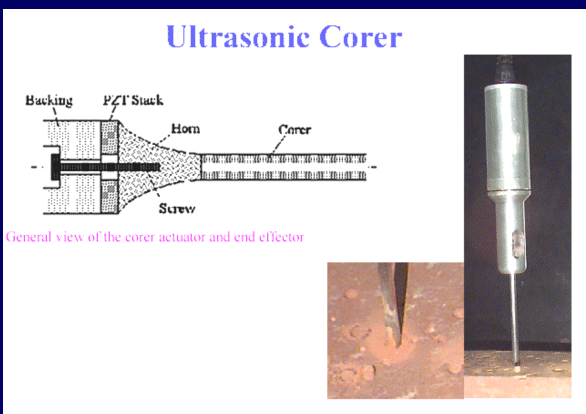

Design by JPL for possible in-situ space application (1998)

Test (Rock)

Ultrasonic Drill Bit, http://eis.jpl.nasa.gov/ndeaa/nasa-nde/usdc/usdc.htm

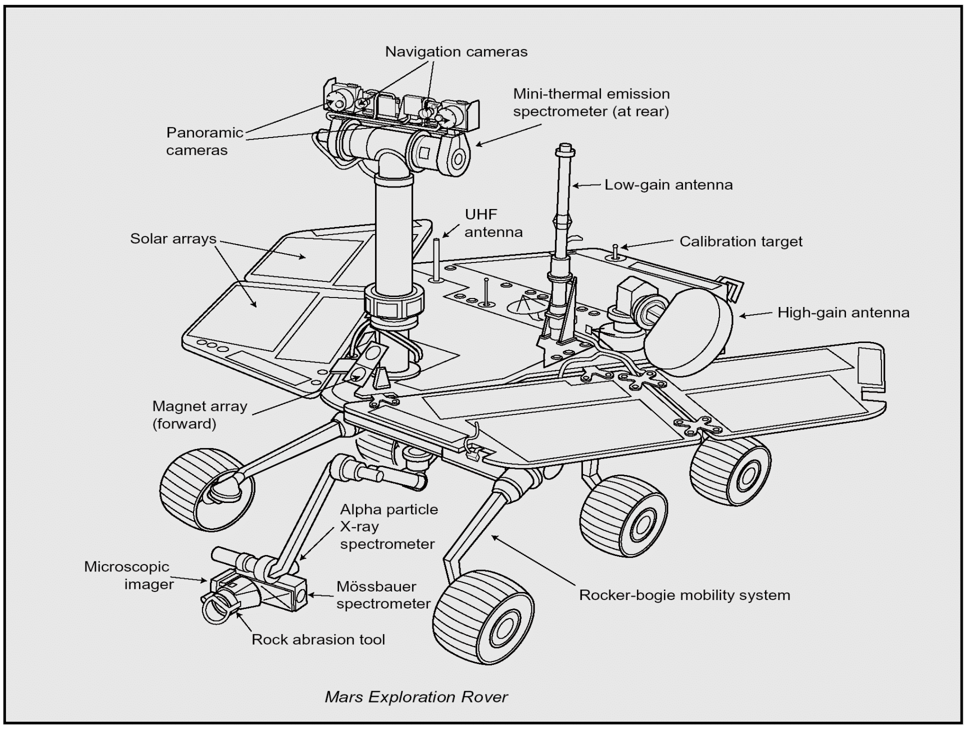

Mars Exploration Rover

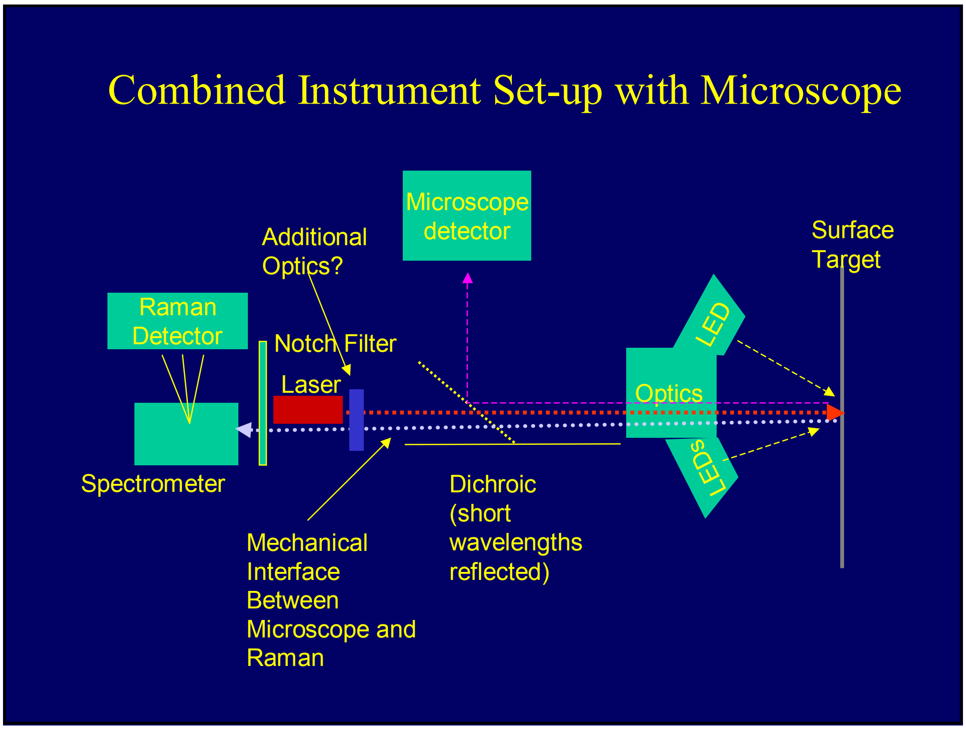

Electrostatic Axially Harmonic Orbital Trapping: A High-Performance Technique of Mass Analysis

A. Makarov 2000

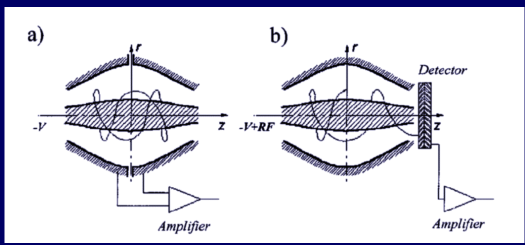

Modes of operation:
a) Fourier transform
b) mass selective instability

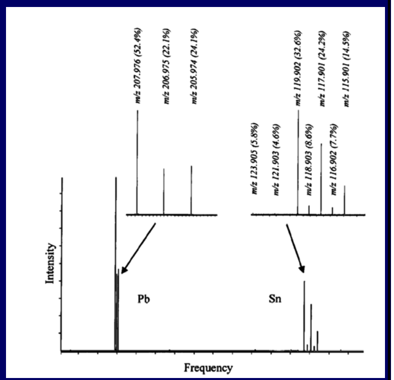

Mass spectrum in frequency domain

Raman spectra of Various Minerals (633nm)

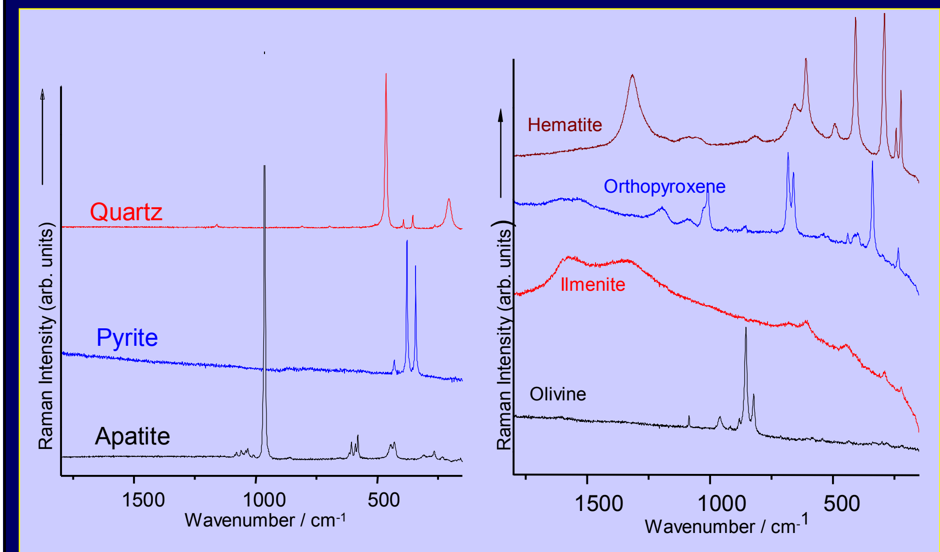

Origin: Formation from nebula dust and gas

(Example: isotopic ratio ^{17}O / ^{16}O and ^{18}O / ^{16}O)

Isotope abundance: The "delta" notation

$\delta^{18}O = ((^{18}O/^{16}O)_{sample} / (^{18}O/^{16}O)_{std} - 1) * 1000$

Example:
The (^{18}O / ^{16}O) $_{std}$ ratio of (SMOW) ***Standard Mean Ocean Water*** is 2.0052 10^{-3}. A sample that is $\delta^{18}O = 5$ heavier than SMOW corresponds to a ratio value of 2.0152 10^{-3}.

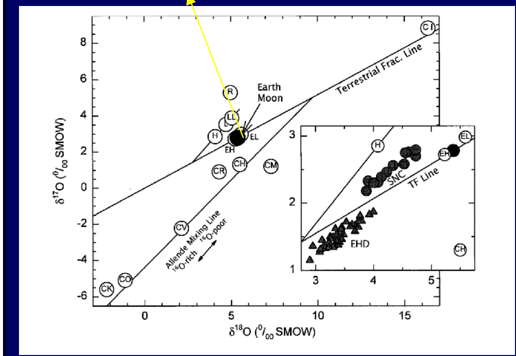

Dynamic range:
about (10^5) to 10^6

High precision required !
Several samples must be analyzed.

Lodders et al. 1997, Clayton et al. 1973

Isotopic ratio: Is the measurement feasible ?

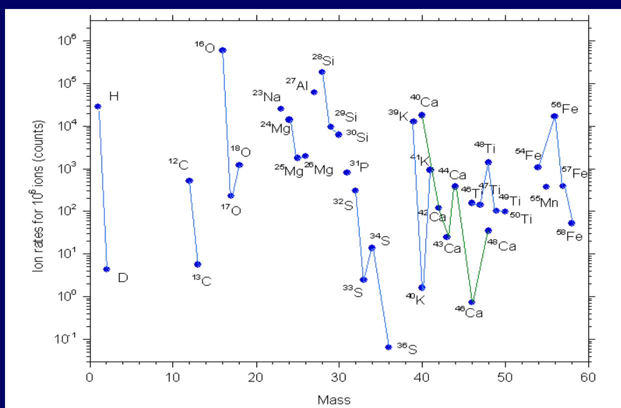

Example: Bulk silicate earth, no fractionation taken into account

The elemental ratio of S to O is comparable to the ratio of the O isotopes:
The requirements for the precision of the elemental abundance measurements could match the requirements of isotopic analysis.

Remote instruments

Remote instruments:
located on orbiting satellites or terrestrial telescopes

Example:

Apollo 15 and 16:
X-Ray Fluorescence and
Gamma-ray Spectrometer

These spectrometer studied the composition of the Moon's surface from lunar orbit. The Gamma-ray Spectrometer was deployed on a 7.6-meter-long boom, visible in the above photograph.

Apollo Gamma-Ray Spectrometer

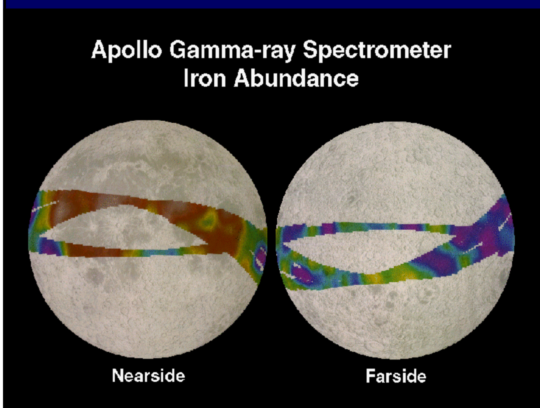

abundences:
red - a high abundance
yellow, green - intermediate
blue, purple - low

resolution:
100 km

Iron abundances

High iron abundances are found in all mare regions
and lower abundances are found elsewhere.

Neutron spectrometer - Mars Odyssey

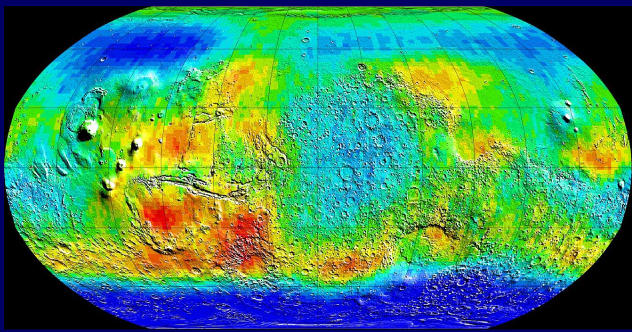

Global Map of Epithermal Neutrons:
Epithermal neutrons provide the most sensitive measure of hydrogen in surface soils. Inspection of the global epithermal map shows high hydrogen content in surface soils south of about negative 60 degree latitude and in a ring that almost surrounds the north polar cap..

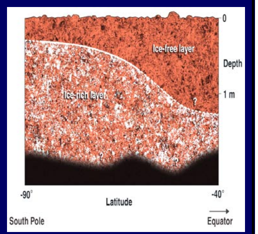

Section of Martian surface

Remote sensing - in-situ measurements

Nanedi Valles system
Mars Global Surveyor
MOC image 8704, 1998
9.6 meters/pixel

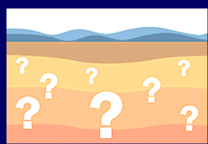

Exploration of soil layers by Sample Acquisition: In-situ Logging and Analysis and / or Sample Return

Mars Rover: Athena